Nuclear Engineering and Technology 55 (2023) 2325–2334

Contents lists available at ScienceDirect

Nuclear Engineering and Technology

journal homepage: www.elsevier.com/locate/net

Original Article

Study on transient performance of tilting-pad thrust bearings in nuclear pump considering fluid-structure interaction

Qiang Li*, Bin Li, Xiuwei Li, Quntao Xie, Qinglei Liu, Weiwei Xu

College of New Energy, China University of Petroleum (East China), Qingdao, 266580, China

ARTICLE INFO

Article history:
Received 4 August 2022
Received in revised form
14 February 2023
Accepted 5 March 2023
Available online 7 March 2023

Keywords:
Nuclear pump
Tilting pad thrust bearings
Fluid-structural interaction
Start-up
User defined function (UDF)
Computational fluid dynamic (CFD)

ABSTRACT

To study the lubrication performance of tilting-pad thrust bearing (TPTBs) during start-up in nuclear pump, a hydrodynamic lubrication model of TPTBs was established based on the computational fluid dynamics (CFD) method and the fluid-structure interaction (FSI) technique. Further, a mesh motion algorithm for the transient calculation of thrust bearings was developed based on the user defined function (UDF).

The result demonstrated that minimum film thickness increases first and then decreases with the rotational speed under start-up condition. The influence of pad tilt on minimum film thickness is greater than that of collar movement at low speed, and the establishment of dynamic pressure mainly depends on pad tilt and minimum film thickness increases. As the increase of rotational speed, the influence of pad tilt was abated, where the influence of the moving of the collar dominated gradually, and minimum film thickness decreases. For TPTBs, the circumferential angle of the pad is always greater than the radial angle. When the rotational speed is constant, the change rate of radial angle is greater than that of circumferential angle with the increase of loading forces. This study can provide reference for improving bearing wear resistance.

1. Introduction

The nuclear main pump is used to drive the coolant to circulate in the RCP (reactor coolant system) system, which is the key to the control of water circulation in nuclear power operation. TPTBs, as a key component of nuclear pump equipment, plays a vital role in the operation of nuclear pump [1,2]. In a typical nuclear pump, the shaft system is usually arranged vertically to minimum the deflection of the shafting, the weight of the rotating parts and the axial hydraulic thrust of the nuclear power runner make the vertical thrust of the collar larger [3]. Thus, the application of TPTBs allows the transfer of loads from sliding components to stationary components through lubricating oil film [4]. Guo et al. [5] considered the state of oil film has a significant influence on the lubrication performance of thrust bearing. Qing et al. [6] further believed that optimizing the state of oil film is always an important research direction of thrust bearing.

Due to the complex structure and operating environment of thrust bearing of nuclear main pump, it is a common practice to simplified bearing and use numerical simulation to calculate the performance of bearings [7,8]. With the development of computational technology, Computation Fluid Dynamics (CFD) method become a popular way to study the oil film flow and pad rotation considering the viscosity shearing heat generation. Jiang et al. [9] studied the effects of load and rotational speed on the film thickness and temperature. Chen et al. [10] used a CFD model to analyze the effects of the pad inclination angle and the rotor speed on the lubrication. Galvão et al. [11]found that the coordinates of the pivot pads variation of a hydrodynamic thrust bearing can result in hydrodynamic pressure field changes that forms on the surface of the pad with consequent changes in the values of the bearing performance parameters, such as power loss, load capacity and temperatures. Wang et al. [12] built a 3D CFD model for the thrust bearing in Three-Gorge hydropower station, and the effects of the oil film clearance size and rotational speed on the load capacity were discussed. Zhai et al. [13] and wodtke et al. [14] used the FSI technique to analyze the thermal-hydro-dynamic (THD) lubrication of thrust bearings and predict the lubrication performance, such as the pressure, temperature. Later, wodtke et al. [15] used FSI method to do a thermal-elastic-hydro-dynamic (TEHD) analysis for a thrust bearing in a hydro power plant, the numerical results are agreed

* Corresponding author.
E-mail address: liq@upc.edu.cn (Q. Li).

https://doi.org/10.1016/j.net.2023.03.007

well with the measurement data, and also demonstrated that the temperature, displacement, heat fluxes and forces were exchanged at the fluid-structure interface between the oil film and the pad. However, the variation of oil film thickness is mainly determined by the pad rotation and collar movement [16], the research on transient motion characteristics of pad under different operating conditions is not enough.

The thrust bearing of nuclear pump is stable when it runs under rated operating condition [17,18], but the collar rotational speed is low during machine start-up and makes oil film difficult to generate sufficient pressure to provide full film lubrication. Therefore, the bearings may fail in the first few minutes of machine start-up , resulting in pad wear [19]. If the nuclear pump fails to start-stop safely, it will not only cause economic losses, but also lead to safety accidents [20]. With the construction of nuclear power units around the world continues to improve, relying on standard steady-state analysis may not provide accurate information about transient performance, because the flow field of the bearing takes at least a few minutes to adapt to new conditions, and operating parameters often change very quickly [21]. The problem of transient flow caused by boundary movement can be solved by meshless method and dynamic mesh method. Compared with the meshless method, the dynamic mesh method is more mature in the study of simulating the flow field changing with time due to the boundary motion [22].

Ettles et al. [23] summarized the research results of various thrust bearing configurations under transient conditions, the result showed that transient effect can cause excessive thermal deformation of pad. Pajaczkowski et al. [24] studied the transient TEHD simulation of hydrodynamic TPTBs in the process of warm and cold start-up with the method of FEM and CFD, the minimum oil film thickness stabilizes almost immediately, while the deformation stabilizes much longer. Li et al. [25] studied the transient effect and oil film thickness of thrust bearing during start-stop process through experimental, the results show that the transient thermal effect and oil film thickness change rapidly at start-up and stop stages, but not obviously at constant speed. Therefore, it is very important for equipment stability design to study the reason of oil film thickness variation in start-up state.

Despite these examples, the influence of operating conditions on pad motion characteristics needs to be systematically analyzed, especially the nuclear pump start-stop process. The study applied the FSI technique to analyze the lubrication performance of TPTBs in a nuclear pump based on the CFD method. The motion boundary of the TPTBs is defined based on the UDF, and macros written in C programming language were loaded into FLUENT through the UDF interface to realize this control. The transient characteristics of the TPTBs are calculated based CFD model. The pad tilt angle and collar movement process under different operating conditions are further analyzed.

2. Methods

2.1. Calculation models

A tilting pad was adopted to increase the load capacity and improve the unit stability of pump. The pads can swing freely with the difference of rotational speed, load and bearing temperature, wedge shape of oil film is formed in the rotational direction and generating higher dynamic pressure. Under the assumption that bearing and collar are perfectly aligned, the calculation results of single pad can be used to predict the performance of the whole bearing.

The point-pivoted TPTBs and details of pads are shown in Fig. 1. Each pad is supported by a point pivot, that allows them to freely

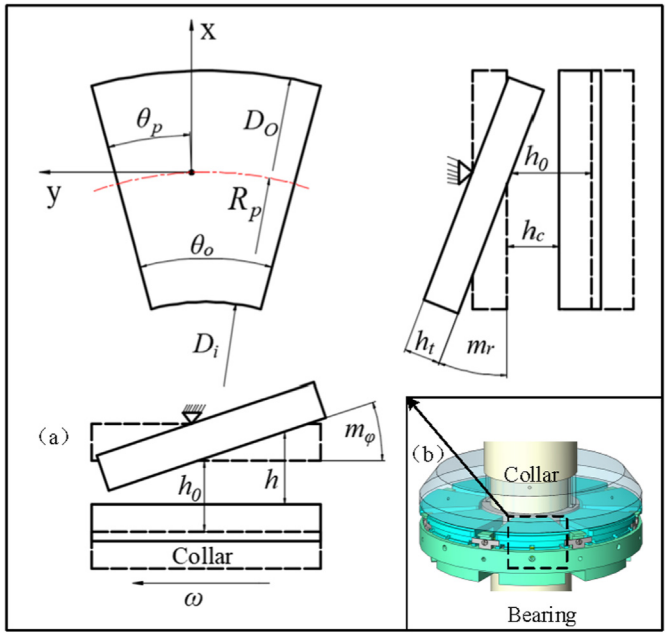

Fig. 1. A point-pivoted TPTBs construction (a) The geometry of the pad and the oil wedge (b) Collar and bearing assembly 3D model.

tilt around a radial line (given by circumferential angle mϕ) and any line (given by radial angle mr). During the operation of bearings, each pad automatically adjusts tilt angle to achieve the film geometry and balance the operating conditions encountered.

As shown in Fig. 2, a three-dimensional model of tilting pad is established and realizes the fluid-structure interaction between the transient flow field and the pads tilt. The pad is considered as a steel body, the gap between the collar and the pad is considered as a fluid domain, and the interface between the solid domain and the fluid domain is set as a coupling surface. The lubricating oil flows in from the left and flows out from the other three sides. The collar is set as the moving wall, the inlet and outlet are set as the pressure inlet and outlet.

The geometric and operating parameters of the pad in the calculation model are presented in Table 1.

2.2. Governing equation

In current studies, fluid flowing is generally considered to be a non-isothermal process, and the minimum pressure value is considered to be higher than the lubricating oil cavitation pressure, that is, the occurrence of cavitation is not considered. In the calculation process of this paper: (1) the bearing is assumed to be laminar flow and the deformation of mirror plate and tile is ignored; (2) The frictional stress in the fluid obeys Newton's law;

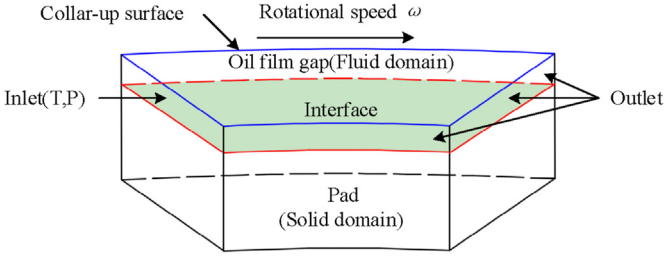

Fig. 2. Three-dimensional model of pad and boundary conditions.

Table 1
Main geometric parameters and operating conditions of pad.

Parameter types	Items	Value
Structural parameters	Outer diameter Do (mm)	690
	Inner diameter Di (mm)	330
	Thrust pad arc angle θo (deg)	30
	Pad thickness ht (mm)	40
	Oil film thickness h0 (mm)	0.2
	Circumferential eccentricity	0.55
	Radial eccentricity	0.569
Operating parameters	Inlet pressure Pin (MPa)	0.3
	Outlet pressure Pout (MPa)	0.1
	Inlet temperature T (°C)	60
	Rotational speed N (r/min)	400–1600
	Angular speed ω (rad/s)	2400–9600

(3) The fluid is single-phase and incompressible.

The continuity equation is given as:

$$\frac{\partial}{\partial t}(\rho)+\nabla\cdot\left(\rho\vec{v}\right)=0 \tag{1}$$

where $\vec{v}$ is the velocity; ρ is the density of the liquid.

The momentum equation is given as:

$$\frac{\partial}{\partial t}\left(\rho\vec{v}\right)+\nabla\cdot\left(\rho\vec{v}\vec{v}\right)=-\nabla\cdot\left[\mu\left(\nabla\vec{v}+\nabla\vec{v}^{T}\right)\right]-\nabla p+S_{\vec{v}} \tag{2}$$

where μ is viscosity of liquid; $S_{\vec{v}}$ is the momentum source term.

$$\frac{\partial}{\partial t}\sum_{k=1}^{n}(\alpha_k\rho_k E_k)+\nabla\cdot\sum_{k=1}^{n}\left(\alpha_k\vec{v}_k(\rho_k E_k+p)\right)=\nabla\cdot\left(k_{eff}\nabla T\right)+S_E \tag{3}$$

where keff is the effective thermal conductivity, SE is the volumetric heat source.

The heat transfer between the fluid and the pad adopts the coupled heat boundary condition, in which the heat conduction of the solid is coupled with the convective heat transfer of the fluid in the calculation process. The temperature distribution in the tilting pad can be calculated by the solid heat conduction equation, which is given by the following Eq. (4).

$$\frac{\partial}{\partial t}(\rho_s h_s)+\nabla\cdot\left(\vec{v}_s\rho_s h_s\right)=\nabla\cdot(k_s\nabla T_s)+S_{hs} \tag{4}$$

The geometry of the pad and the oil wedge are shown in Fig. 2. The oil film thickness is composed of two parts: the basic geometry of the oil film gap and the displacement of the collar. Thus, the oil film thickness can be calculated by Eq. (5).

$$\begin{aligned} h_i &= h_o-h_c-h_t \\ h_t &= \sin m_r\left[R_P-r\cos(\theta-\theta_p)\right]+\sin m_\phi r\sin(\theta-\theta_p)\end{aligned} \tag{5}$$

where hc is the displacement of collar, ht is the displacement of pad, θp is the angle between the oil inlet edge and the pivot point. Rp is the radius of pivot.

The viscosity of lubricating oil decreases with the increase of lubricating oil temperature. The lubricating oil is ISO VG 32 oil, the change of viscosity with temperature can be predicted by Walther formula.

$$\mu_l=\rho_t[10\hat{1}0\hat{[}A-B\log(T-273.15)]-0.7] \tag{6}$$

The parameters A, B and physical parameters of the lubricating oil are shown in Table 2.

Table 2
Viscosity and temperature performance parameters of lubricating oil.

ISO VG 32	A	8.5922
	B	3.3705
	Density ρ (kg/m3)	850
	Dynamic viscosity μ40/μ100 (Pa•s)	0.0272/0.00527

2.3. Grid independence

The grid size has little effect on the calculation results in the circumferential and radial directions, being less than 0.4% and 0.3%, respectively. In the axial direction, for clearance of the oil film (the clearance between the collar and the pad), the number of grid divisions may lead to significant calculation deviation, as shown in Table 3. The grid result is shown in Fig. 3.

2.4. The transient model and dynamic mesh updating algorithm

The movement of the collar and the pad tilt changes the structure of the bearing lubrication flow field, resulting in the variation of the lubrication flow field pressure, the temperature of the pad and other parameters. In the bearing system, the collar is affected by the force of gravity produced by the rotor mass and external load. Hence, the establishment of dynamic oil film in bearing clearance is a transient flow process caused by boundary motion.

When the oil film force Fo on the collar is equal to the external load force Fe, and the position of the collar remain stable, it can be considered to be in equilibrium. The oil film force Fo on the surface of the collar is calculated by Equation (7):

$$F_o=\oiint sp_o dxdy \tag{7}$$

where s is the area, po is the oil pressure.

$$\frac{d}{dt}(mv)=(F_o-F_e) \tag{8}$$

where v is the axial movement velocity of the mirror plate.

The infinitesimal body is taken from the steel body, and the force analysis is carried out on it, as shown in Fig. 4. The resultant torques of the pad in different directions can be calculated by UDF integration. The torques in different directions are calculated by Equation (9).

$$\begin{cases} M_o(F)_x=(y-y_o)F_{oz}-(z-z_o)F_{oy} \\ M_o(F)_y=(z-z_o)F_{ox}-(x-x_o)F_{oz} \\ M_o(F)_z=0 \end{cases} \tag{9}$$

where Mop(F) is the resultant moment on the pad; (xo, yo, zo) is the coordinate of the pivot point; Fox, Foy and Foz are the oil film forces in x, y and z-directions, respectively.

The rotation of the thrust pad around the pivot point is determined by the moment of force acting on the thrust pad. The motion of the tilting pad can be obtained from Equation (10):

$$\begin{cases} \frac{d}{dt}J_{ox}\omega_x=M_{ox}(F)_x \\ \frac{d}{dt}J_{oy}\omega_y=M_{oy}(F)_y \end{cases} \tag{10}$$

where Jox and Joy is the moment of inertia of the pad to the pivot; ωx and ωy is the angular velocity of the pad.

The transient calculation process is shown in Fig. 5. Firstly, the surface pressure of the collar is integrated to obtain the transient oil film force, and the displacement of the shaft under the current time

Table 3
Verification of axial grid independence of oil film clearance.

Grid quantity	Axial grid layers	Maximum oil film pressure (MPa)	Deviation (%)	minimum oil film thickness (μm)	Deviation (%)
523328	3	3.394	1.39	113.25	−3.39
537472	4	3.421	0.61	112.13	−2.37
551616	5	3.435	0.20	110.74	−1.10
565760	6	3.442	reference	109.532	reference

Note: Radial: 120 divisions; axial: 6 divisions; circumferential: 220 divisions.

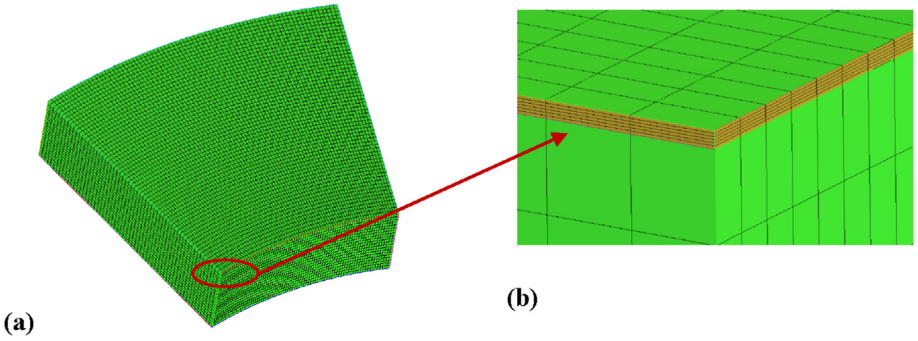

Fig. 3. Model grid (a) Grid distribution; (b) Grid of fluid domain.

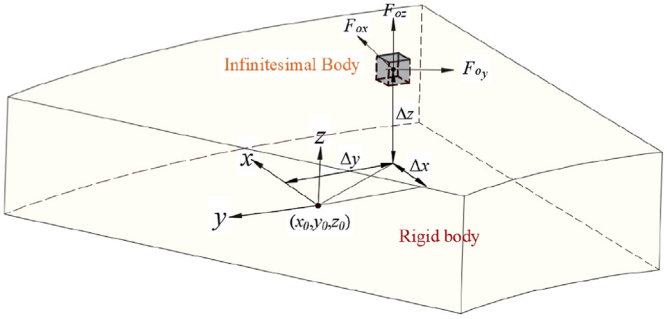

Fig. 4. Force analysis of steel body.

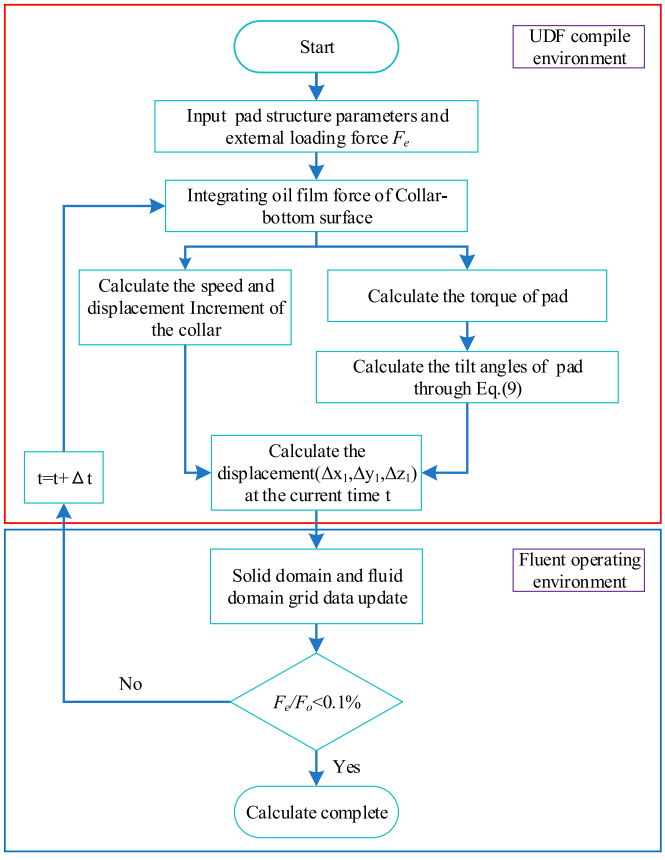

Fig. 5. Transient calculation process.

step is calculated. Then, the surface pressure of each pad is integrated, and the tilt angle of each tilt pad within the current time step is calculated according to Equation (10). Finally, a UDF is used to complete the motion of the mirror plate and the fixed-point rotation of the thrust pad.

The dynamic mesh methods provided by FLUENT include smoothing, layering and remeshing. Among the three methods, layering and remeshing will result in the generation and disappearance of grid nodes [26]. In the smoothing method, the motion of the boundary is absorbed by the internal nodes, there is no generation or disappearance of grid nodes in the process of mesh deformation. For the CFD model of thrust bearing, a standard dynamic mesh updating method cannot avoid the computational difficulties caused by mesh distortion in transient calculation [27]. The algorithm is based on compiled user defined functions (UDFs) and can be used for transient calculation of bearings in FLUENT.

The fluid domain and solid domain are divided into structural grids based on the ICEM software, the dynamic grid program developed by ourselves is used in CFD software FLUENT to realize the precise movement of grid node. The total number and topology relationship of the grid nodes remain the same during the calculation process. After all nodes are looped over at time level, their coordinates are all known and can be precisely calculated again at time level t+Δt. During the transient calculation process, after iterations, the mesh after updating control by the UDF can maintain high quality. The grid deformation at a certain time step is shown in Fig. 6(b), which is a 2D simplified model with a greatly enlarged small clearance to better display the grid.

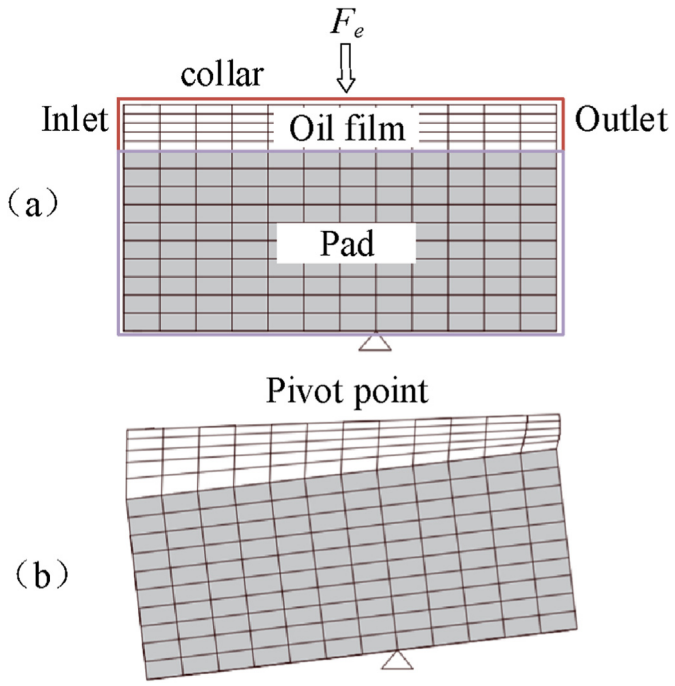

Fig. 6. local grid update process; (a) Initial grid (t = 0) (b) Grid updated.

3. Model validation

In discrete solution of the governing equation, a double precision solver is used to avoid the influence of excessive aspect ratio of the grid, SIMPLE algorithm is used in the pressure-velocity coupling algorithm. When the residual value of the continuity equation is reduced to 10−5 and the loading force is approximately equal to the oil film force, the calculation is considered to converge.

In order to verify the validity of the transient model developed in this paper, the simulated results are compared with Deng et al. [28]. The bearing parameters are shown in Table 4. The minimum film thickness is taken as the key parameter to consider the lubrication performance of the bearing. Fig. 7 shows the comparison of minimum film thickness based on the different method, and the maximum error of different models is about 15%. Therefore, the model in this paper is feasible.

4. Result and discussion

4.1. Influence of start-up conditions on bearing performance

The start-up lubrication performance of thrust bearing plays a vital role in the stable operation of nuclear main pump. Therefore, the study of transient performance provide reference for bearing design and improve the bearing loading capacity. The axial force of rotor system is changing constantly during start-up. The lubrication performance of bearings was studied under the nuclear pump coolant system pressure of 2.4 MPa and 2.8 MPa respectively, and the transient motion process of collar and pad are further analyzed.

$$F_S = p_s \cdot \frac{\pi}{4} d^2 \tag{11}$$

where ps is nuclear pump coolant system pressure, d is the rotor diameter. Fs is pressure acting on shaft seal.

$$\sum F_e = -G + F_S - F_H \tag{12}$$

$$F_H = k\rho g H \frac{\pi\left(D_2^2 - d_n^2\right)}{4} \tag{13}$$

where G is weight of rotating parts, FH is axial thrust of hydraulic components and is variating with the system temperature and speed of impeller.

Fig. 8 shows the variation of loading force Fe with rotational speed under different coolant system pressures. Under the start-up condition, the loading force increases as the increase of rotational speed.

The minimum oil film thickness was calculated at coolant system pressure of 2.4 MPa and 2.8 MPa, as shown in Fig. 9. Surprisingly, the minimum oil film thickness changes nonlinearly, but increases first and then decreases with the increase of rotational speed. When the rotational speed is 600 r/min, the minimum film thickness reaches the maximum. When the pressure is 2.4 MPa and 2.8 MPa, the maximum of minimum oil film thickness is 56 μm and 63 μm, respectively.

In order to explain the reason for the change of oil film thickness under the start-up conditions, the circumferential angle and radial angle change with the rotational speed as shown in Fig. 10. As the rotational speed increases, the tilt angle gradually decreases, and the tilt angle in a stable state at 1600r/min. According to Eq. (5), the change of film thickness is determined by the displacement of collar and the tilt of pad. The displacements caused by the collar movement and pad tilt at the pressure of 2.4mpa and 2.8mpa are given in Fig. 8. When the rotational speed is less than 600 r/min, the influence of pad tilt on minimum film thickness is greater than that of collar movement due to the large tilt angle of pad, and the minimum film thickness increases gradually (h400<h500<h600). That is, the establishment of dynamic pressure at low speed mainly depends on pad tilt. When the rotational speed is greater than 600 r/min, the influence of pad tilt on minimum film thickness is less than that of collar movement due to the small tilt angle, and the oil film thickness decreases gradually (h600>h800, etc). Therefore, the establishment of dynamic pressure under high speed mainly depends on the moving of the collar. Some special designs must be used to avoid side effects in transient situations with the insufficient load-carrying capacity (see Fig. 11).

The calculated pressure and temperature profiles at the start-up pressure of 2.4mpa and 2.8mpa is shown in Fig. 12, the trends of variation in the maximum pressure and maximum temperature are similar. As the speed increases, the high-pressure area of the oil film gradually shifts from the outlet area to the pivot point position as shown in Fig. 12(a). The maximum pressure under 2.4 MPa is larger than 2.8 MPa condition due to the higher loading forces. Similarly, the maximum temperature of the thrust pad increases with the rotational speed, the decrease of film thickness at the inlet, which resulting in a reduction in lubricant flow rate. In addition, the decrease of oil film thickness leads to the enhancement of shear effect and the friction heat, the maximum temperature under 2.4 MPa is larger than 2.8 MPa, as shown in Fig. 12(b).

Table 4
Bearing parameters.

Parameter	Value
Main/Reverse bearing outer diameter (mm)	370/401
Main/Reverse bearing inner diameter (mm)	775/652
Main/Reverse bearing pad angle (deg)	40.54°/27.26°
Type of lubricating oil	ISO VG 32

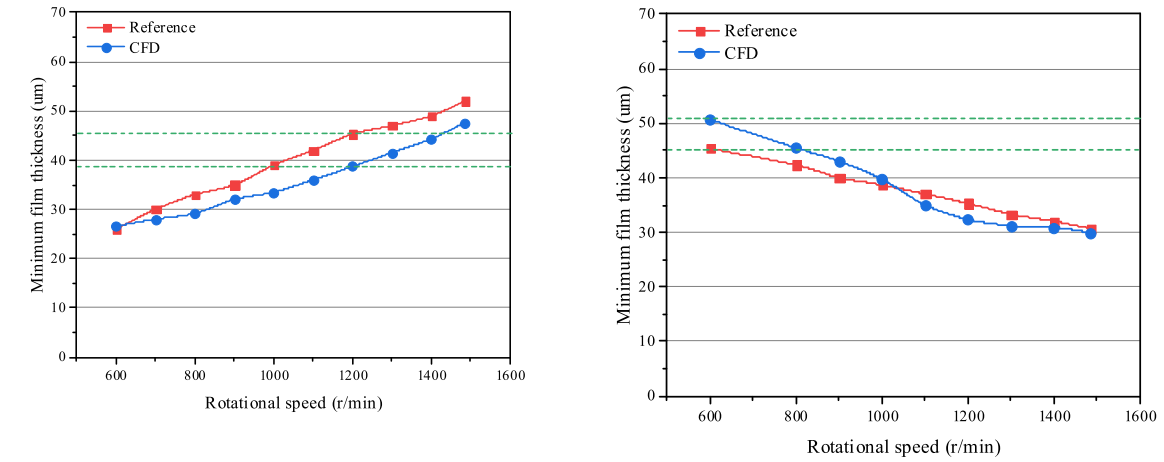

a Comparison of minimum film thickness of main bearing

b Comparison of minimum film thickness of reverse bearing

Fig. 7. Comparison of minimum oil film thickness of bearing under different geometric parameters.

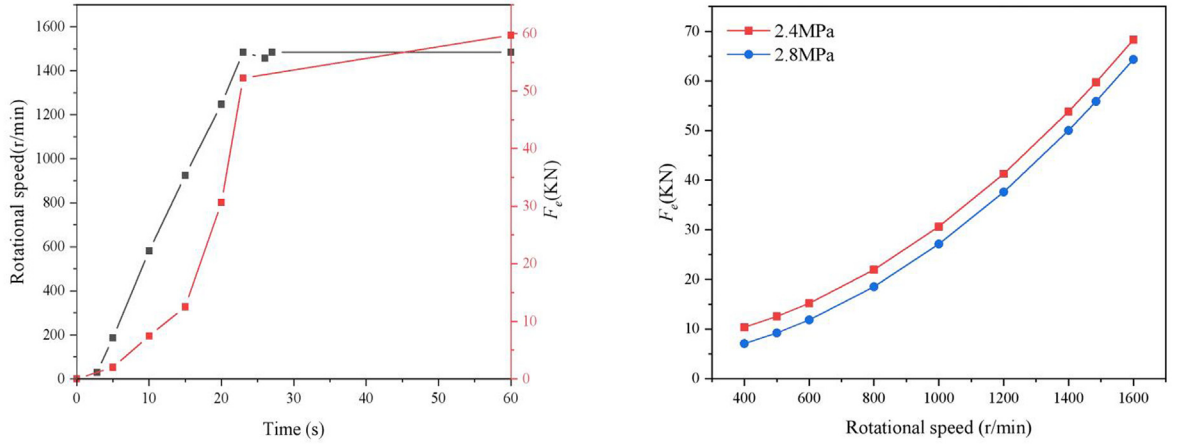

a Variation of operating condition parameters with time(2.4MPa)

b Variation of loading force F_e

Fig. 8. Operating parameter.

4.2. *Influence of loading force on bearing characteristics*

In order to demonstrate the effect of loading force on the lubrication characteristics of thrust bearings, such as pressure, temperature and oil film thickness. Table 5 shows the loading force Fe under different coolant system pressure when the rotational speed of nuclear pump is 1485r/min.

Fig. 13 shows the oil film pressure distribution on the pad under different loading force, the pressure distribution of oil film under different loading forces is very similar. As the loading force increases, the high-pressure area is shifted towards the opposite direction of rotation, the pressure outside the thrust pad area is very small, meaning that the pressure in the membrane is much higher than the pressure of the oil inlet.

The temperature distribution of the pad under different Fe is shown in Fig. 14. The temperature at the lubricating oil inlet is low, and the highest temperature is distributed at the oil outlet near the outer diameter of the pad. That is due to the large linear velocity at the outer diameter and the viscous friction of the oil film, the temperature of the pad near the back edge is much higher than that of the leading edge.

The oil film thickness distribution of the thrust pad under different Fe is shown in Fig. 15. The maximum film thickness is at the lubricating oil inlet, and the thickness decreases circumferentially at the right exit outer diameter and reaches the minimum at the right exit outer diameter.

In summary, the maximum pressure shifts to the pivot point of pad, and the temperature of pad increases circumferentially with the increase of Fe. At the outer diameter of the right exit, the maximum linear velocity and the minimum thickness of the lubricating oil result in the strongest shear flow, which leads to the highest friction heat flux and temperature. The thickness of oil film decreases, the pressure of oil film increases, and the shear flow strength increases, which leads to the increase of temperature. However, the higher the temperature, the lower the viscosity of the oil and the lower the pressure, so the loading force and oil film force are balanced by reducing the film thickness.

Fig. 16 shows the motion of the pad under different loading forces. Under the same loading force, the circumferential angle of pad is always larger than the radical angle. The bearing gives the oil film a wedge shape in the direction of rotation and generates higher

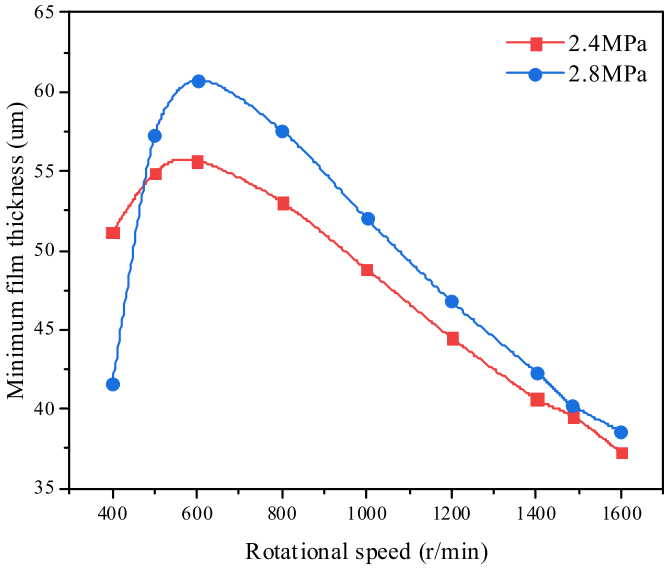

Fig. 9. Minimum oil film thickness.

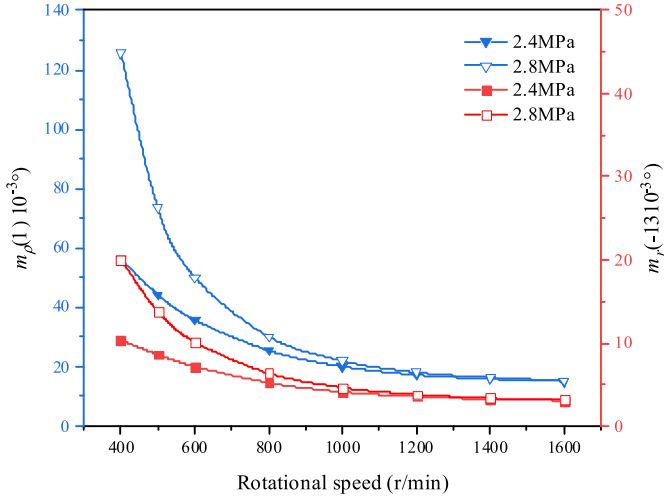

Fig. 10. Tilt angle of pad transient rotation.

dynamic pressure to balance the external load. The shape of the oil wedge is mainly determined by the tilt angle along the x-direction, which increases the lubricating oil inlet clearance, as shown in Fig. 16(a). In addition, with the increase of the loading force, the tilt angle and the minimum oil film thickness of the pad decrease simultaneously, which means that there are two ways to balance the larger loading force of the bearing system: the decreases of the overall oil film and the pad tilt angle. The initial tilt angle of pad varies rapidly and the bearing can establish dynamic pressure in a relatively short time. Under the action of centrifugal force, the oil is brought to the outside of the pad, which increases the radical angle along y-direction, as shown in Fig. 16(b).

Fig. 17 shows the variation of the ratio of the circumferential angle to the radical angle with time under different loading forces. When N = 1485r/min, as the increase of the loading force, the tilt angle of the pad decreases in both directions, and its ratio increases. Meanwhile, as the loading force increases, the circumferential angle of the pad decreases slightly along the x-direction, and the radical angle of the pad decreases greatly along the y-direction. The effect of radical angle on bearing performance is more pronounced

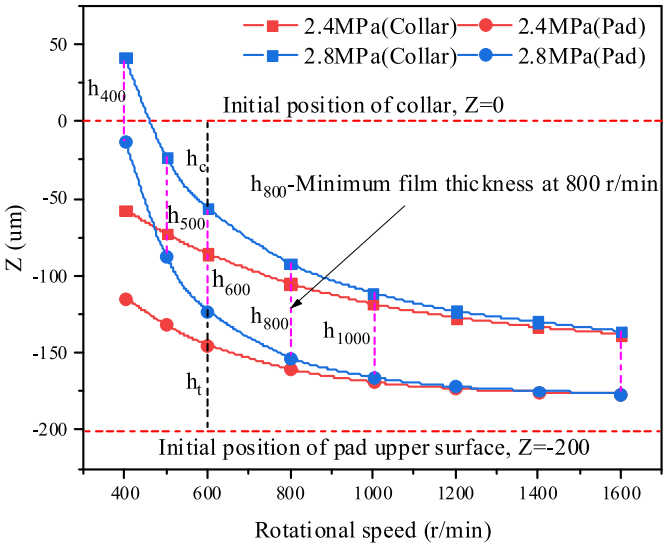

Fig. 11. Variation the displacement of collar and pad.

with the increase of loading force. Further, the increase of loading forces will lead to substantial reduction of the circumferential angle, resulting in the reduction of minimum film thickness, and the film thickness is mainly determined by the circumferential angle. The lubrication requirements of thrust bearing system can be achieved by adjusting the tilt angle of pad.

5. Conclusions

The purpose of the present paper is to investigate the transient performance of bearings based on the computational fluid dynamics method (CFD). The bearing mechanism of TPTBs under different working conditions is explained, and predict the effect of nuclear pump start-up on the lubrication performance of thrust bearings under different coolant system pressure. It provides theoretical support for improving bearing wear resistance and bearing optimization design. The main conclusions are as follows.

1) The three-dimensional hydrodynamic lubrication model of TPTBs was established based on the CFD method and the FSI technique. Further, a mesh motion algorithm for the transient calculation of thrust bearings was proposed based on the User Defined Function (UDF). The validity of the calculation model was verified.
2) When the nuclear pump is in the start-up condition, and the coolant system pressure is 2.4Mpa and 2.8Mpa, the high-pressure area of the oil film gradually moves from the oil outlet edge to the pivot point, and the maximum pressure increases continuously. The maximum temperature is at the oil outlet near the outer diameter of the pad and decreases gradually along the circumferential. Minimum film thickness increases and then decreases with increasing of rotational speed, the influence of pad tilt on minimum film thickness is greater than that of collar movement at low rotational speed. The establishment of dynamic pressure at low speed mainly depends on pad tilt. The opposite conclusion is reached at high rotational speed.
3) When the rotational speed is 1485 r/min, the maximum oil film pressure and the maximum temperature of the pad increase with the increase of loading force, and the minimum oil film thickness decreases. Circumferential angle is always greater than radial angle as the dynamic pressure builds up, and

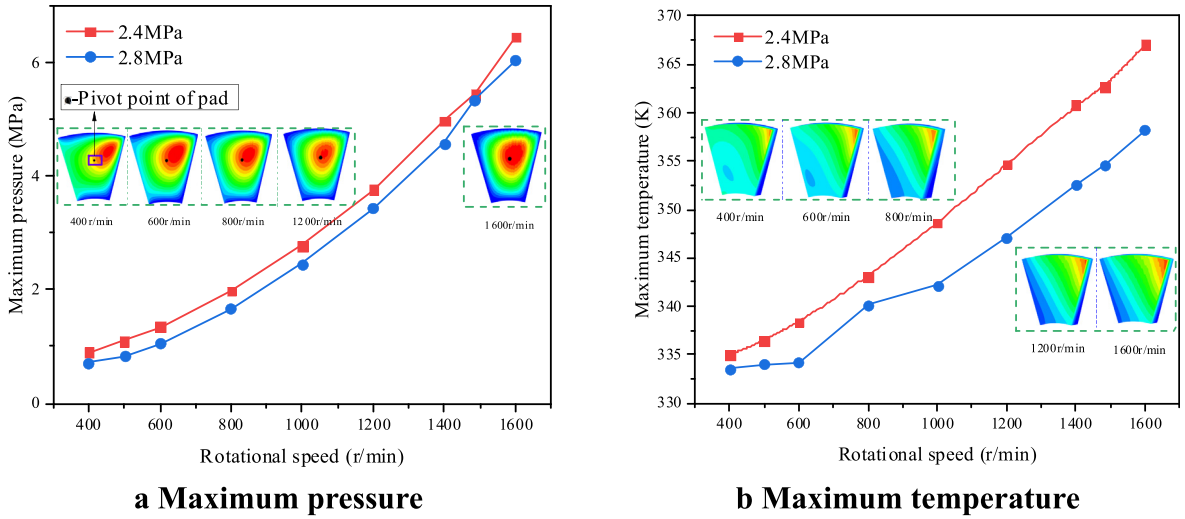

Fig. 12. Variation of lubrication parameters under start-up conditions.

Table 5
Loading forces at 1485 r/min.

Rotation speed N (r/min)	Coolant system pressure ps (MPa)	Load force Fe (KN)
1485	2.4	477
1485	2.8	447
1485	7	176

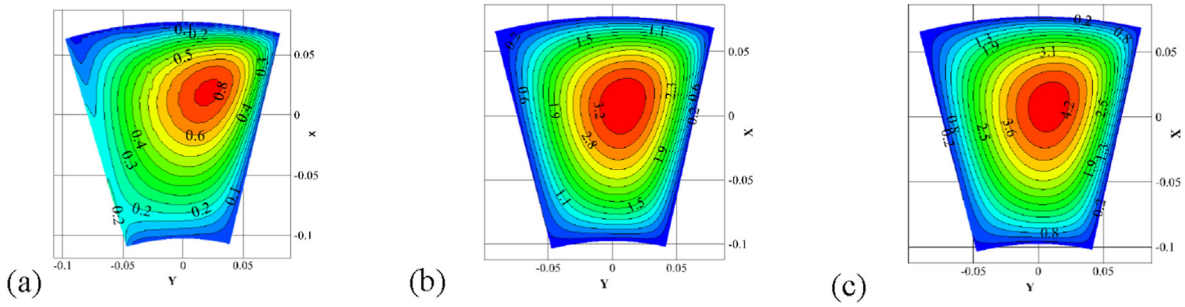

Fig. 13. Contour plot of hydrodynamic pressure (MPa) (a)176 KN, 1485r/min, (b) 447 KN, 1485r/min, (c) 477 KN, 1485r/min.

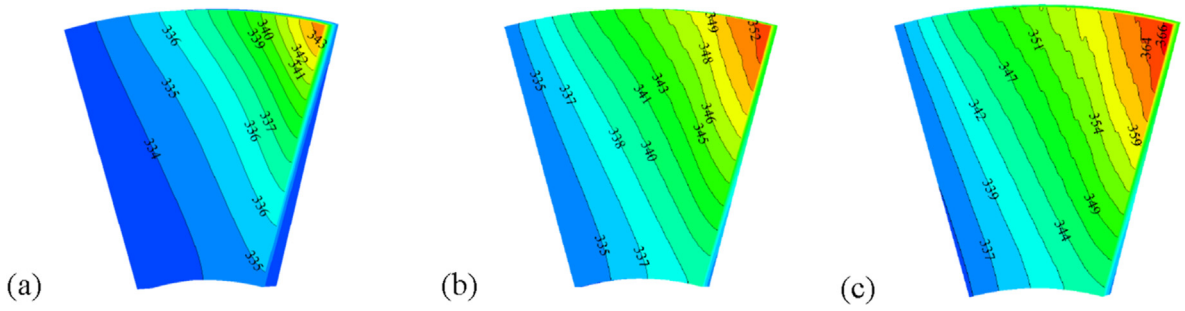

Fig. 14. Contour plot of pad temperature (K) (a)176 KN, 1485r/min, (b) 447 KN, 1485r/min, (c) 477 KN, 1485r/min.

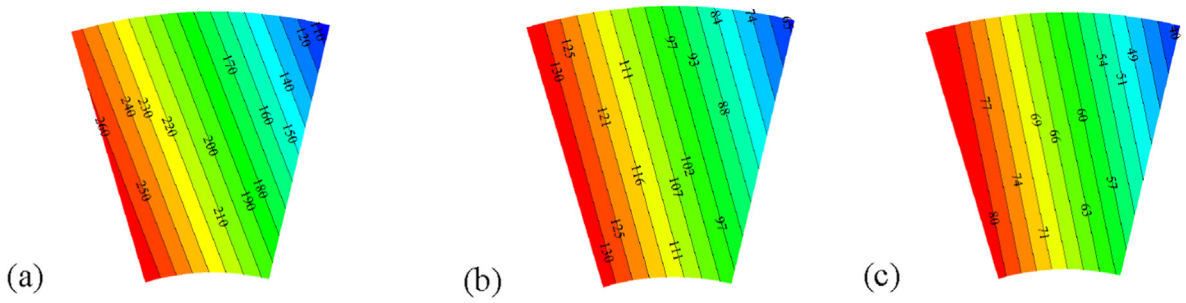

Fig. 15. Contour plot of oil film thickness (um) (a)176 KN, 1485r/min, (b) 447 KN, 1485r/min, (c) 477 KN, 1485r/min.

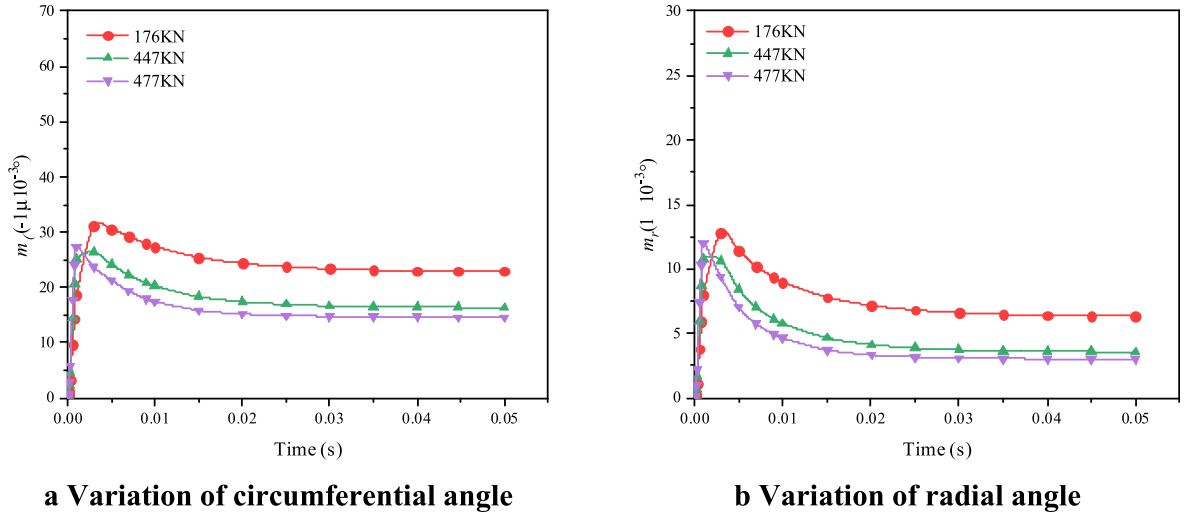

Fig. 16. Tilt angle of pad, N = 1485r/min.

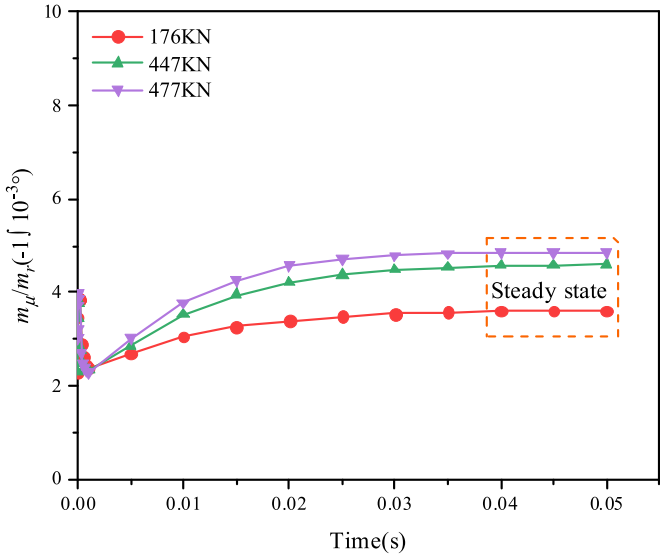

Fig. 17. Variation of the ratio of the circumferential angle to the radical angle, N = 1485r/min.

through the analysis of the ratio of the circumferential angle to the radial angle, it is found that the effect of radial angle on establishment of dynamic pressure is more pronounced with the increase of loading force.

Declaration of competing interest

The authors declare that they have no known competing financial interests or personal relationships that could have appeared to influence the work reported in this paper.

Acknowledgements

This work was supported by the National Natural Science Foundation of China (NO. 52176050, NO. 51506225), the General Program of Natural Science Foundation of Shandong Province (NO. ZR2020ME174).

References

[1] R. Liu, L. Jing, X. Meng, B.G. Lyu, Mixed elastohydrodynamic analysis of a coupled journal-thrust bearing system in a rotary compressor under high ambient pressure[J], Tribol. Int. 159 (2021), 106943.
[2] T.F. Peixoto, K.L. Cavalca, Thrust bearing coupling effects on the lateral dynamics of turbochargers, Tribol. Int. 145 (2020), 106166.
[3] Y.M. Mo, Y. Gong, Z.G. Yang, Failure analysis on the O-ring of radial thrust bearing room of main pump in a nuclear power plant, Eng. Fail. Anal. 115 (2020), 104673.
[4] Y.A. Radin, I.A. Grishin, Axial thrust balancing in high-temperature cylinders of steam turbines during transients in combined-cycle units, Appl. Therm. Eng. 66 (2019) 409–414.
[5] A.N. Guo, X.J. wang, J. Jin, D.Y. Hua, Z.K. Hua, Experimental test of static and dynamic characteristics of tilting-pad thrust bearings, Adv. Mech. Eng. 7 (2015), 1687814015593878.
[6] W. Ouyang, X.Y. Yuan, Q. Jia, Analysis of tilting-pad thrust bearing static instability and lubrication performance under the bistability, Ind. Lubric. Tribol. 66 (2014) 584–592.
[7] Q. Zhou, H.K. Li, L. Pei, Z.W. Zhong, Research on non-uniform pressure

pulsation of the diffuser in a nuclear reactor coolant pump, Nucl. Eng. Technol. 53 (2021) 1020–1028.
[8] X.G. Guo, Y. Li, Z.J. Jin, R.K. Kang, Modeling and simulating of high chromium alloy based on molecular dynamics, J. Nanosci. Nanotechnol. 19 (2019) 4671–4676.
[9] X. Jiang, J. Wang, J. Fang, Thermal elastohydrodynamic lubrication analysis of tilting pad thrust bearings, Proc. Inst. Mech. Eng. Part J.-J. Eng. Tribol. 225 (2011) 51–57.
[10] R.L. Chen, X.Z. Wang, C. Du, J.L. Wang, J. Zha, K. Liu, Study on the influence of thrust plate tilt on performance of distributed hybrid thrust bearing with tilting pad, J. Braz. Soc. Mech. Sci. Eng. 43 (2021) 320.
[11] M.M. Galvão, G.J. Menon, V.A. Schwarz, Numerical study of the influence of the pivot position on the steady-state behavior of tilting-pad thrust bearings, J. Braz. Soc. Mech. Sci. Eng. 39 (2017) 3165–3180.
[12] H.J. Wang, R.Z. Gong, D.P. Lu, Z.D. Wu, F.C. Li, Numerical simulation of the flow in a large-scale thrust bearing, in: 3rd Joint US-European Fluids Engineering Division Summer Meeting, Canada, Montreal, Aug 1-5, 2010.
[13] L. Zhai, Y. Luo, X. Liu, F.A. Chen, Y.X. Xiao, Z.W. Wang, Numerical simulations for the fluid-thermal-structural interaction lubrication in a tilting pad thrust bearing, Eng. Comput. 34 (2017) 1149–1165.
[14] M. Wodtke, A. Olszewski, M. Wasilczuk, Application of the fluid–structure interaction technique for the analysis of hydrodynamic lubrication problems, Proc. Inst. Mech. Eng. Part J.-J. Eng. Tribol. 227 (2013) 888–897.
[15] M. Wodtke, A. Schubert, M. Fillon, M. Wasilczuk, P. Pajaczkowski, Large hydrodynamic thrust bearing: comparison of the calculations and measurements, proceedings of the institution of mechanical engineers, Proc. Inst. Mech. Eng. Part J.- J. Eng. Tribol. 228 (2014) 974–983.
[16] L.M. Zhai, Y.Y. Luo, Z.W. Wei, X. Liu, Y.X. Xiao, A review on the large tilting pad thrust bearings in the hydropower units, Renew. Sustain. Energy Rev. 69 (2017) 1182–1198.
[17] C.M. Ettles, J. Seyler, M. Bottenschein, Calculation of a safety margin for hydrogenerator thrust bearings, Tribol. Trans. 48 (2005) 450–456.
[18] L. Zoupas, M. Wodtke, C.I. Papadopoulos, M. Wasilczuk, Effect ofmanufacturing errors of the pad sliding surface on the performance of the hydrodynamic thrust bearing, Tribol. Int. 134 (2019) 211–220.
[19] B. Pap, M. Fillon, M. Guillemont, L. Bauduin, J. Chocron, P. Gédin, L. Biadalla, Experimental and numerical analysis on the seizure of a carbon-filled PTFE central groove journal bearing during start-up period, Lubricants 6 (2018) 14.
[20] L. Cai, W.G. Wang, M.K. Lei, M.Q. Li, B. Zhu, X.S. Su, Study on wear mechanism of thrust bearing of nuclear main pump in cooling water loss condition, Nucl. Power Eng. 42 (2021) 214–221.
[21] Z.C. Wang, F. Guo, Y. Liu, X.F. Liu, Y.M. Wang, Asymmetry characteristic of tilting-pad thrust bearing during the start-up and shut-down process, Ind. Lubric. Tribol. 70 (2018) 1806–1814.
[22] M.X. Li, C.H. Gu, X.H. Pan, S.Y. Zheng, Q. Li, A new dynamic mesh algorithm for studying the 3D transient flow field of tilting pad journal bearings, Proc. Inst. Mech. Eng. Part J.- J. Eng. Tribol. 230 (2016) 1470–1482.
[23] C.M. Ettles, J. Seyler, M. Bottenschein, Some effects of start-up and shut-down on thrust bearing assemblies in hydro-generators, J. Tribol. Trans. ASME 125 (2003) 824–832.
[24] P. Pajączkowski, A. Schubert, M. Wasilczuk, M. Wodtke, Simulation of large thrust-bearing performance at transient states, warm and cold start-up, Proc. Inst. Mech. Eng. Part J.-J. Eng. Tribol. 228 (2013) 96–103.
[25] P.J. Li, Y.S. Zhu, Y.Y. Zhang, Z. Chen, Y.P. Yan, Experimental study of the transient thermal effect and the oil film thickness of the equalizing thrust bearing in the process of start-stop with load, Proc. Inst. Mech. Eng. Part J.-J. Eng. Tribol. 227 (2013) 26–33.
[26] Y.Q. Zhang, Z.Q. Zhang, X.B. Kong, R. Li, Application of dynamic mesh technology in the oil film flow simulation for hydrostatic bearing, Ind. Lubric. Tribol. 71 (2019) 146–153.
[27] V. Meruane, R. Pascual, Identification of nonlinear dynamic coefficients in plain journal bearings, Tribol. Int. 41 (2008) 743–754.
[28] X. Deng, Y. Wang, L. Deng, Y.F. Mao, N. Zhao, J. Liu, Analysis of dynamic characteristics of thrust bearing for nuclear power plant RCP during loss of power coastdown, Nucl. Power Eng. 38 (2017) 50–54.